# Supporting Information

## IL-functionalized Mn(II) -doped core-shell $Fe_3O_4$@ Zr-MOF nanomaterials for removal MB from wastewater based on dual adsorption/Fenton catalysis

Ruowei Lu, [a] Cuijuan Wang, [a] *Yanxia Chen, [a] Lichuan Tan, [a] Peng Wang, [a] and Siwen Feng [a]

[a] Department of Chemistry and Chemical Engineering, School of Life Science and Engineering, Southwest Jiaotong University, Chengdu, Sichuan, 610031, PR China

*Corresponding Author

### Figures and tables

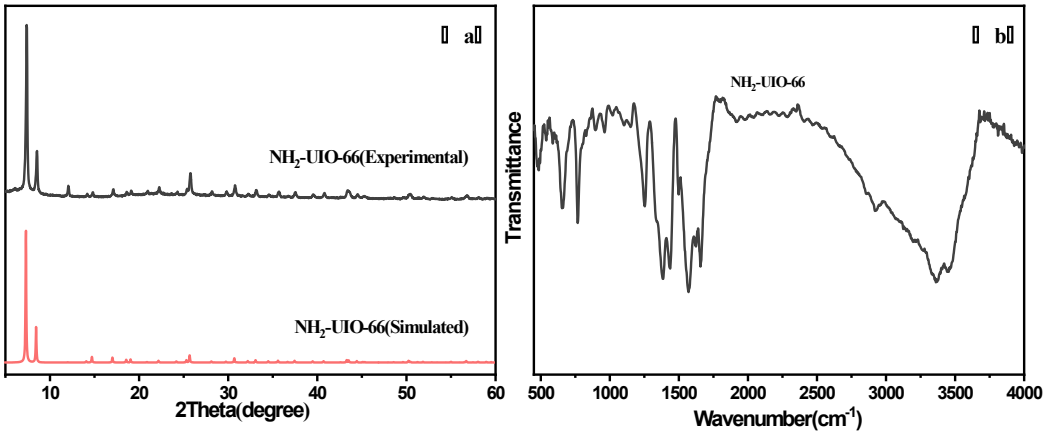


Figure. S1. (a) PXRD patterns and (b) FT-IR spectra of $NH_2$-UiO-66.

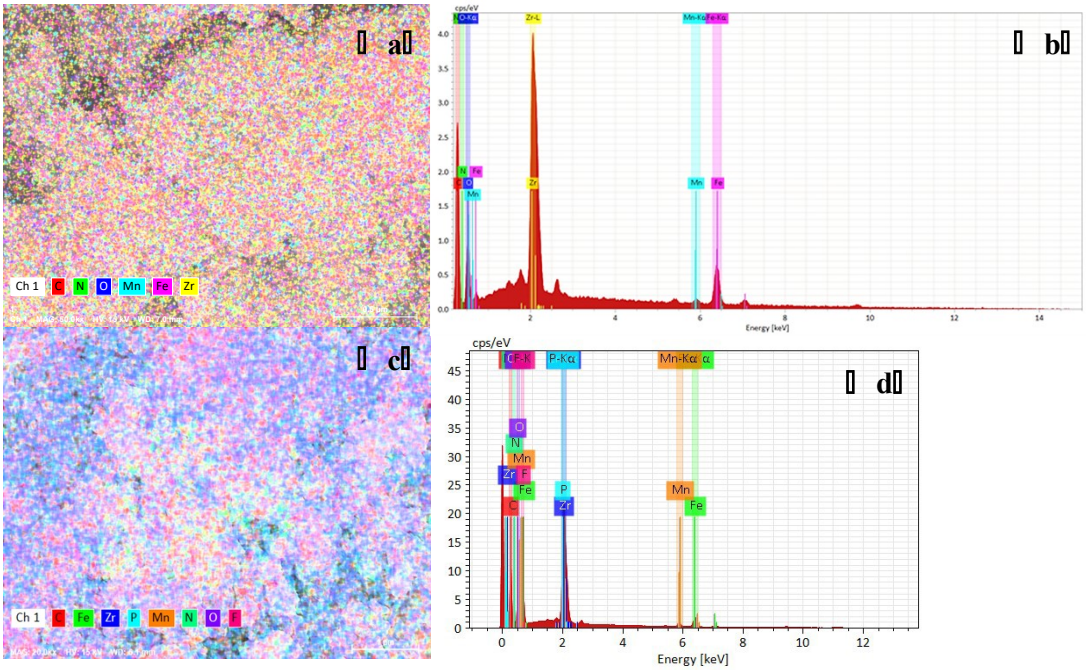


Figure. S2. EDS spectrum of the obtained MFC@Mn-$NH_2$-UiO-66 and MFC@Mn-$NH_2$-UiO-66@IL magnetic composites.

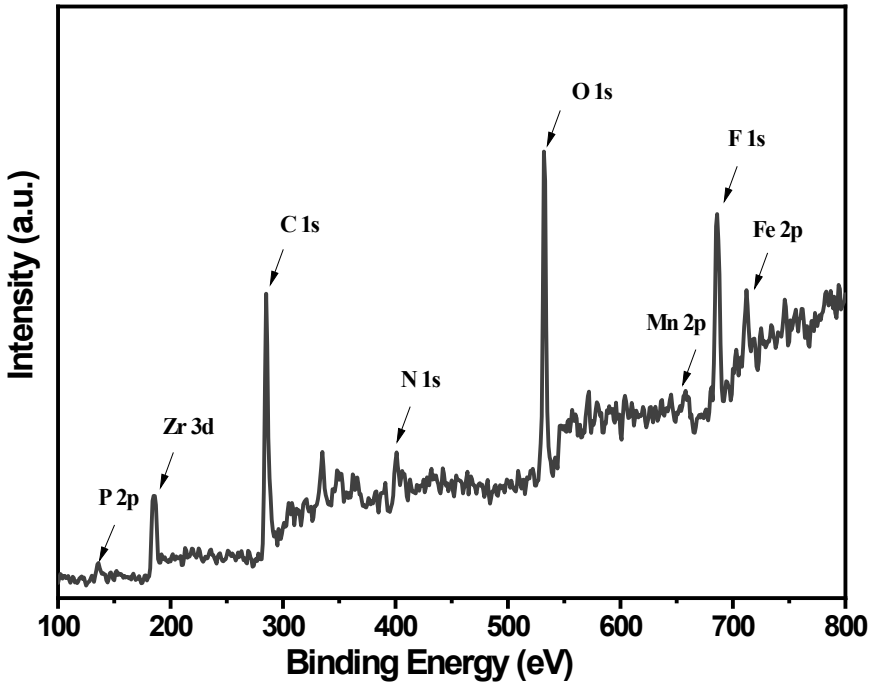


Figure. S3. XPS spectra of MFC@Mn-$NH_2$-UiO-66@IL.

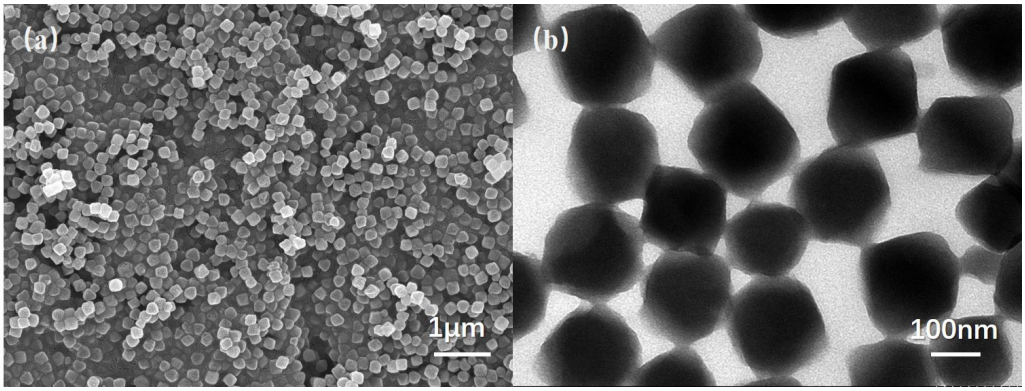


Figure. S4. (a) SEM and (b) TEM images of $NH_2$-UiO-66.

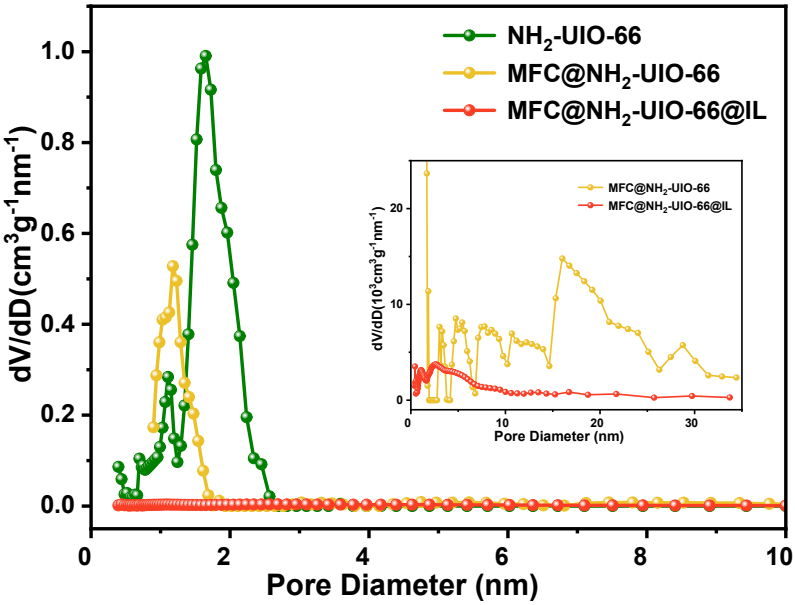


Figure. S5. The pore size distribution of $NH_2$-UiO-66, MFC@Mn-$NH_2$-UiO-66 and MFC@Mn-$NH_2$-UiO-66@IL nanocomposites.

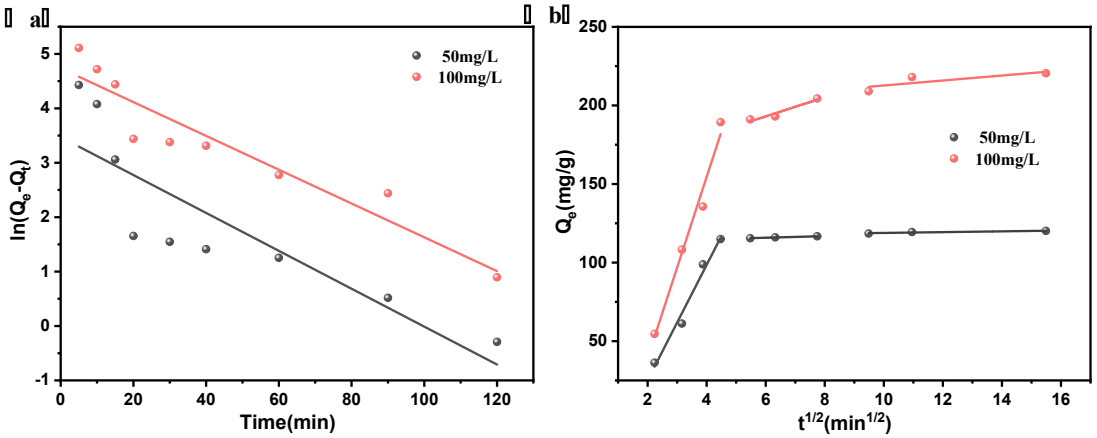


Figure. S6. (a) Kinetics plot of the pseudo first-order, and (b) intra-particle diffusion kinetic model for MB adsorption.

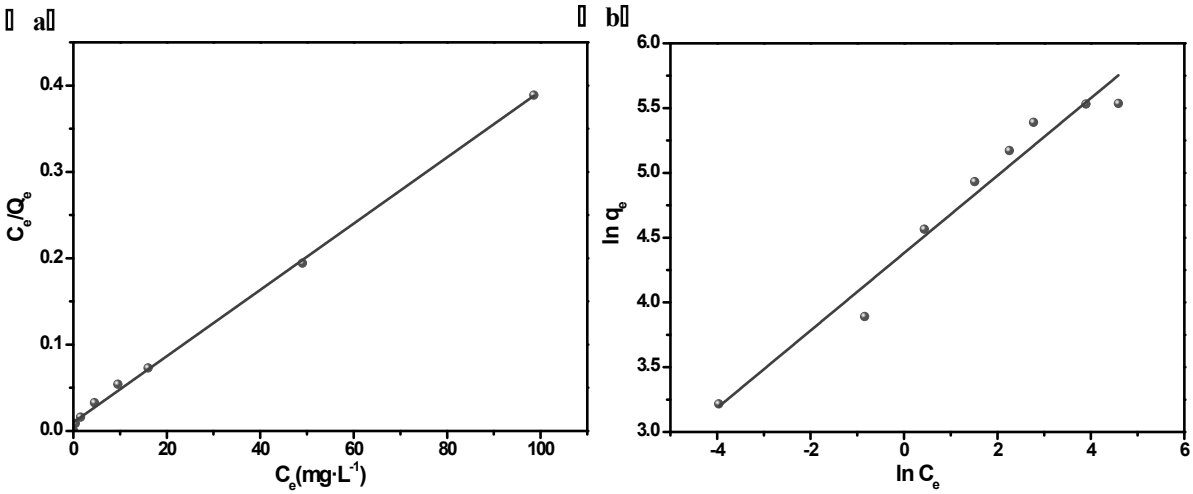


Figure. S7. Adsorption isotherm of (a) Langmuir, and (b) Freundlich model for MB removal by MFC@Mn-$NH_2$-UiO-66@IL.

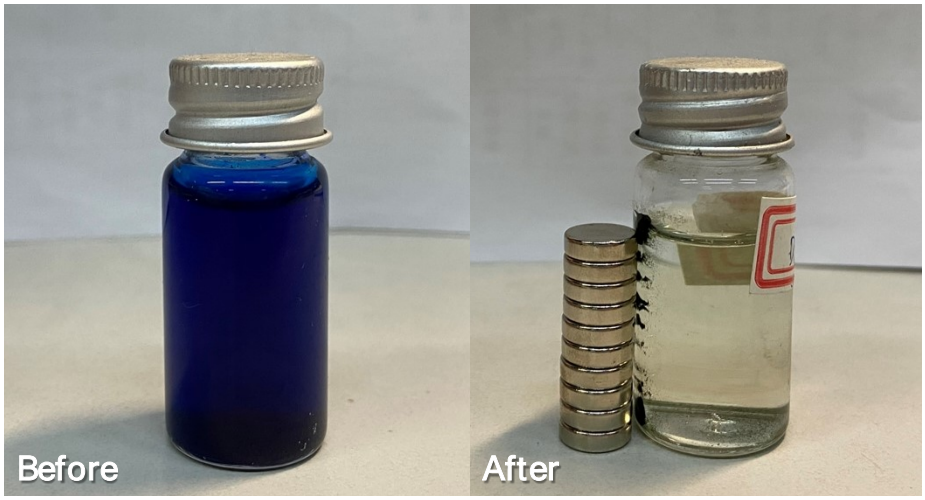


Figure. S8. Before and after comparison of adsorption/catalytic MB.

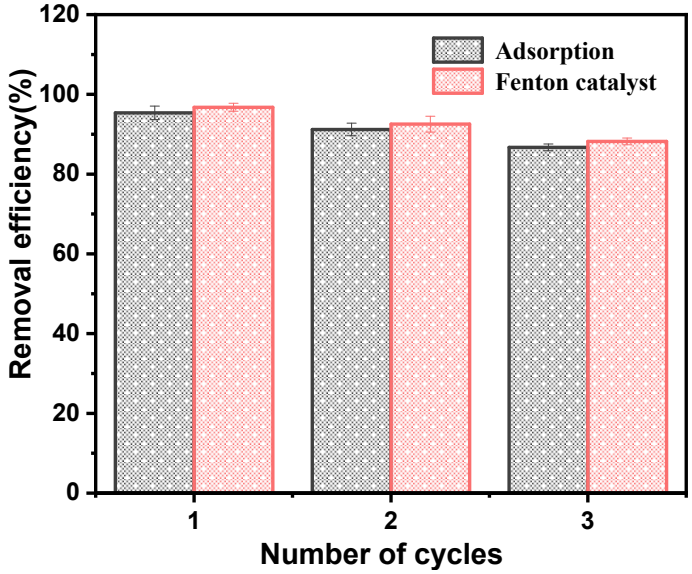


Figure. S9. Recycle efficiency of MFC@Mn-$NH_2$-UiO-66@IL over three cycles.

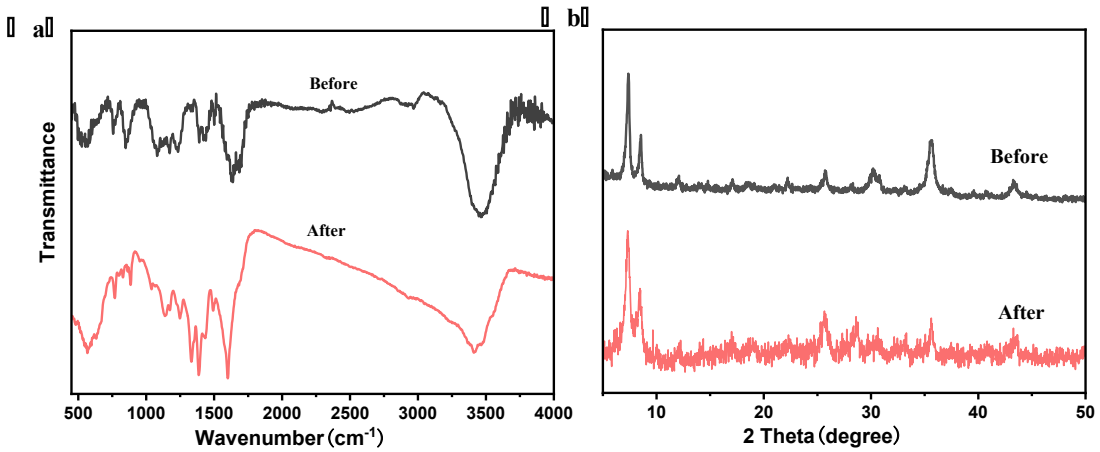


Figure. S10. (a)FT-IR spectra and (b)PXRD patterns MFC@Mn-$NH_2$-UiO-66@IL composite before and after adsorption of MB.

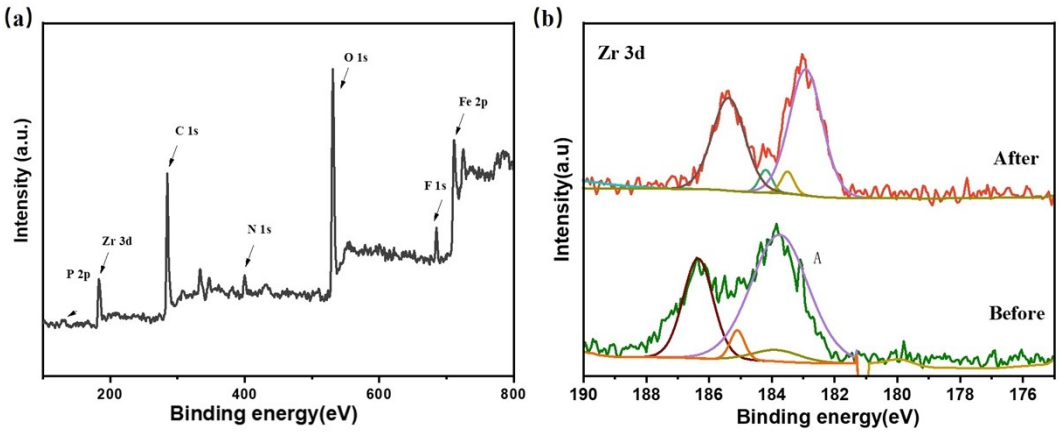


Figure. S11. XPS spectra of the recycled MFC@Mn-$NH_2$-UiO-66@IL: (a) The survey spectrum; (b) XPS Zr 3d spectrum.

Table. S1. Element components of MFC@Mn-$NH_2$-UiO-66, and MFC@Mn-$NH_2$-UiO-66@IL.

| Samples | C (wt%) | Zr (wt%) | O (wt%) | F (wt%) | Fe (wt%) | N (wt%) | P (wt%) | Mn (wt%) |
|---|---|---|---|---|---|---|---|---|
| MFC@Mn-$NH_2$-UiO-66 | 41.51 | 24.46 | 15.95 | - | 11.4 | 4.07 | - | 1.05 |
| IL@MFC@Mn-$NH_2$-UiO-66 | 31.21 | 23.28 | 21.62 | 7.68 | 6.41 | 7.44 | 1.53 | 0.66 |

Table. S2. BET surface areas and t-plot micropore volumes of samples.

| Samples | $S_{BET}(m^2 \cdot g^{-1})$ | $V_{pore}(cm^3 \cdot g^{-1})$ |
|---|---|---|
| $NH_2$-UiO-66 | 1264.30 | 0.54 |
| MFC@Mn-$NH_2$-UiO-66 | 699.25 | 0.46 |
| MFC@Mn-$NH_2$-UiO-66@IL | 30.31 | 0.06 |

Table. S3. Intra-particle diffusion model parameters for the adsorption of MB dye onto MFC@Mn-$NH_2$-UiO-66@IL composite

| $C_0(mg \cdot L^{-1})$ | First step | | | Second step | | | Third step | | |
|---|---|---|---|---|---|---|---|---|---|
| | $K_{id,1}$ (mg $g^{-1}min^{-0.5}$) | $C_1$ ($mg \cdot L^{-1}$) | $R^2$ | $K_{id,2}$ (mg $g^{-1}min^{-0.5}$) | $C_2$ ($mg \cdot L^{-1}$) | $R^2$ | $K_{id,2}$ (mg $g^{-1}min^{-0.5}$) | $C_3$ ($mg \cdot L^{-1}$) | $R^2$ |
| 50 $mg \cdot L^{-1}$ | 57.69 | -76.25 | 0.98 | 6.09 | 196.86 | 0.67 | 1.58 | 156.48 | 0.94 |
| 100 $mg \cdot L^{-1}$ | 36.72 | -48.33 | 0.98 | 0.51 | 116.35 | 0.88 | 0.25 | 112.72 | 0.98 |

Table. S4. $R_L$ values for the adsorption of MB dye.

| $C_0(mg \cdot L^{-1})$ | 10 | 20 | 40 | 60 | 80 | 100 | 150 | 200 |
|---|---|---|---|---|---|---|---|---|
| $R_L$ | 0.20 | 0.11 | 0.06 | 0.04 | 0.03 | 0.025 | 0.016 | 0.012 |